Digest Journal of Nanomaterials and Biostructures Vol. 6, No 4, October-December 2011, p. 1649-1656

OPTICAL AND MORPHOLOGICAL PROPERTIES OF POLYROTAXANES BASED ON FLUORENE/BITHIOPHENE COPOLYMERS WITH PERSILYLATED β-CYCLODEXTRIN

A. FARCAS*, E. G. HITRUC
"P. Poni" Institute of Macromolecular Chemistry, 41A Gr. Ghica Voda Alley, Iasi-700487, Romania

An alternating conjugated polyrotaxane (**3c**) and its non-complexed homologue (**3**) consisting of 2,2'-bithiophene/persilylated β-cyclodextrin (PS-βCD) and 9,9-dioctylfluorene moieties has been prepared using Suzuki coupling reaction. The optical and morphological properties of **3c** polyrotaxane were analyzed by UV-Vis, fluorescence, atomic force microscopy analysis (AFM), and compared with **3** the non-rotaxanes ones. As a film, **3** exhibits UV-Vis and photoluminescence maxima at 495 and 553 nm, while **3c** at 496 and 524 nm, respectively with blue to green light emission. Polyrotaxane **3c** has a sharper emission spectrum with one peak compared with two peaks of **3**, denoting a quenching effect of the environment induced through the protection of the polymer chain by the PS-βCD macrocycle. Thus, the band gap of **3** and **3c**, estimated from the absorption onset of the UV-Vis spectrum of the polymer film, approximately 2.32 and 2.29 eV, respectively is smaller than that of common polyfluorene (PF) homopolymers. AFM of **3c** sample showed lower values of the root mean square roughness (RMS) (8.9 nm) and the average height profile (28.7 nm), compared with **3** the non-rotaxanes ones. This provides microscopic evidence for strongly reduced interchain interactions, which allows the polyrotaxane to pack densely.

(Received September 15, 2011; accepted October 20, 2011)

Keywords: Fluorene-bithiophene copolymer, Persilylated β-cyclodextrin, Fluorescence, Roughness

1. Introduction

Conjugated polymers attracted much attention as a new class of active organic materials for optoelectronic applications [1-4]. The most advantage of these carbon-based materials over inorganic semiconductors is solution processability and tunability of the optical properties and a unique opportunity for understanding an effective nanoscale control of intermolecular interactions [2]. In the paste decade, fluorene-based conjugated polymers (PFs) attracted a great interest as very promising candidates for blue light-emitting diodes due to their pure blue and efficient luminescence combined with high mobility, excellent thermal and chemical stability, good film-forming and hole-transporting properties [4-9]. Taking into account the required photophysical properties, PFs, the most investigated light-emitting polymer, various strategies to reduce aggregates, and/or excimer formation in the solid state have been investigated [4]. One of the frequently used methods is the copolymerization of fluorene monomers with various aryl comonomers, resulting in enhanced macroscopically photophysical properties. The synthesis of alternating copolymers of 9,9-disubstitued fluorene with electron rich bithiophene or thiophene monomers through Suzuki coupling reaction was found to produce materials with blue to green light emission and good thermal stability but the control over the aggregation and the luminescence quenching by impurities in the solid state of these polymers was not achieved [10-15].

* Corresponding author: auricafarcas@yahoo.com

The main aspects which require optimization from an application point of view are high charge mobility along the individual polymer chains, a smooth morphology of the produced films, and, to the degree that optical applications are concerned, strong fluorescence.

Supramolecular chemistry has produced a variety of rotaxane or polyrotaxanes architectures relevance to optical applications. In the rotaxane architecture, the cyclic molecules (hosts) encapsulate the conjugated polymer backbone (guests) via non-covalent interactions, which helps to minimize the inter-chain interactions/aggregation of the polymers resulting in their improved photophysical properties [16-20]. Among the known host molecules, cyclodextrins (CDs) and their derivatives are the most studied due to their ability to form inclusion complexes with a large variety of low molecular weight compounds or polymers. In general, native CDs can form aggregates in water [21], whereas some of their derivatives, does not display significant aggregation [22]. Previously, interlocked molecules with different structures threaded by cyclodextrins (CDs) or their derivatives as macrocyclic molecules were synthesized and their electro-optical properties have been reported [23-30].

The present study was preformed to explore the opportunities for tuning optical and morphological properties of conjugated polymers by using PS-βCD, as macrocycle molecules. Thus, a main chain polyrotaxane copolymer poly[2,7-(9,9-dioctyl)-*alt*-5,5'-bithiophene/PS-βCD] (**3c**), has been synthesized by using palladium catalyzed Suzuki coupling reaction from 5,5'-dibromo-2,2'-bithiophene as inclusion complex with PS-βCD (**2c**) and a bulky molecule 9,9-dioctylfluorene-2,7-trimethylene diborate (**1**) (Scheme 1). The influence of partially protected bithiophene-fluorene copolymer by PS-βCD in rotaxane architecture on the photophysical and morphological properties, were discussed in detail and compared with the reference sample, a non-rotaxane poly[2,7-(9,9-dioctyl)-*alt*-5,5'-bithiophene] (**3**).

The study is motivated by the potential use of the conjugated polyrotaxanes as thin films for electronic devices.

2. Experimental

2.1. Materials

PS-βCD was obtained by the silylation of native βCD with 1-trimethylsilylimidazole [31]. As appropriate comonomers, which would be able to build through Suzuki coupling [32] the **3c** rotaxane copolymer, a 1/1 **2c** inclusion complex precursor and **1** was chosen. In order to compare the optical and morphological properties induced by the rotaxane architectures when PS-βCD is used as host macrocycle, a reference copolymer **3** was also synthesized by coupling **1** with non-complexed **2**. Copolymers having stable phenyl groups at the end chains with structures presented in Scheme 1 were obtained by adding a slight excess of **1** at the end of polymerization to introduce ester groups at both polymer chain ends, and, finally, terminating the polycondensation with bromobenzene. The detailed procedure and characterization will be reported elsewhere.

^{1}H-NMR (CD_2Cl_2) δ: 7.36-7.67 (m, 6 H from fluorene); 7.24-7.30 (m, 4H from bithiophene); 3.45-4.13 and 5.06 (PS-βCD); 0.79-2.1 (alkyl groups); 0.00 (PS-βCD).

FTIR (KBr, cm^{-1}): 3430, 3060, 2960, 2925, 2854, 1735, 1673, 1606, 1466, 1415, 1256, 1163, 1145, 1086, 1029, 843, 796, 721, 692, 473.

2.2. Characterization

Polymer analysis was performed by ^{1}H-NMR spectrometry (Bruker Advance 400 MHz, in CD_2Cl_2). FTIR analyses of the powder polymers were performed in a Specord Carl Zeiss Jena FTIR spectrophotometer. For FTIR analysis, the samples were prepared by the potassium bromide disc method and scanned within from 4000–400 cm^{-1}. The molecular weights of reference copolymer **3** and **3c** polyrotaxanes were determined by size exclusion chromatography (SEC) in CH_2Cl_2 by using a Water Associates 440 instrument and polystyrene calibrating standards. The surface profile of the polymeric films was evaluated by atomic force microscopy (AFM). AFM measurements were performed in air, at room temperature, in the tapping mode using a Scanning

Probe Microscope with commercially available NSG10 cantilever (Solver PRO-M, NTMDT, Russia). The manufacturer's value for the probe tip radius is 10 nm and the typical force constant is 11.8 N/m. The resonance frequency for this setup was 258 kHz. For image acquisition and analysis the last version of the NT-MDT NOVA software was used. Films of **3** or **3c** copolymers were prepared by spin-coating from CH_2Cl_2 solutions at 3000 rpm for 60 s on a WS-400B-6NPP-Lite Single Wafer Spin Processor (Laurel Technologies Corporation, USA). Absorption spectra were measured on a Specord 200 spectrophotometer in $CHCl_3$ solution and thin films. Fluorescence spectra were obtained with a Perkin Elmer LS55 luminescence spectrophotometer.

3. Results

3.1. Synthesis and characterization

A polyrotaxane based on PS-βCD, **3c**, and its size-persistant non-rotaxane copolymer, **3**, were synthesized through Suzuki coupling reaction [32] between **1** and **2** or **2c**, respectively, as shown in Scheme 1. Theoretically, the alternating coupling reaction of **1**, a bulky group as demonstrated by semiempirical calculations [25], and **2c** inclusion complex can give polyrotaxanes containing a blocking group in each structural unit of the main chain.

The structure of both the rotaxane and non-rotaxane copolymers was proved by ^{1}H-NMR, and FT-IR spectroscopy.

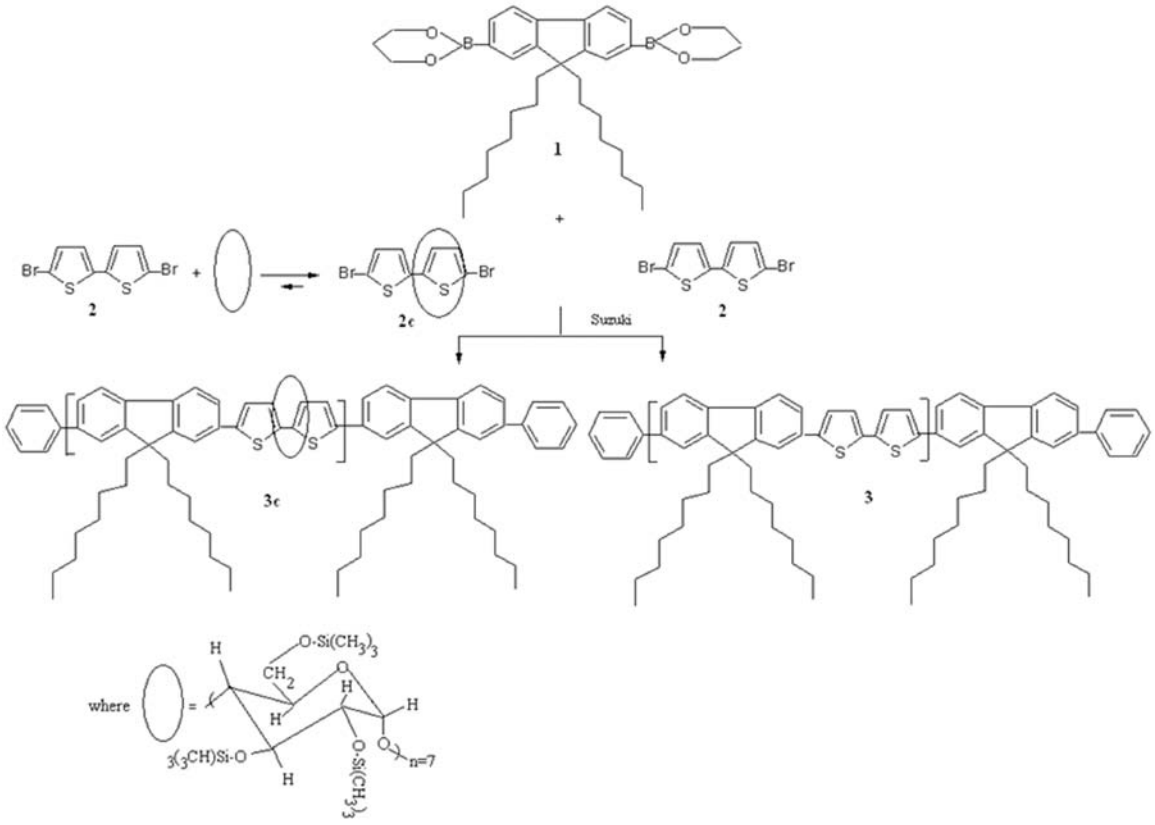

Scheme 1. Synthetic route to the monomers (1, 2c or 2) to 3 and 3c copolymers

The ^{1}H NMR spectrum (not shown) showed only a 32% coverage with PS-βCD macrocycle calculated from the ratio of the integrated area of the peak, assigned to the Si-CH_3 protons of PS-βCD (0 ppm) and a protons assigned to the monomer **2** (7.24-7.30 ppm). The resulting **3c** polyrotaxane (quantified by ^{1}H NMR), suggesting that about every 3rd structural unit was threaded with a macrocycle. This proved that PS-βCD includes the monomer **2** inside much better compared with previously reported results [23].

The determined molecular weights for the **3** and **3c** copolymers, obtained by SEC analysis, are given in Table 1. The observed higher molecular weights for **3c** rotaxane copolymer can be attributed to the positive influence of PS-βCD on the solubility of the **3c** rotaxane copolymer in the reaction medium. The polydispersity (M_w/M_n) values of **3c** (1.84) was higher than that of **3** (1.46), which is presumably due to a compositional polydispersity of the macromolecular chains (variations in the average number of PS-βCD units per chain). The peak of free PS-βCD was not present in the chromatogram of rotaxane copolymer (not shown) and this point evidenced that the rotaxane sample is not a physical mixture between components. Also, The SEC trace of **3c** polyrotaxane copolymer does not show any peak at lower elution volume attributed to the aggregation of the macromolecular chains behaviour reported for other rotaxane polymers [26].

Note that the molecular weights of the conjugated polymers obtained have to be taken as indicative only, since calibration with polystyrene may induce questionable results when the polarity and backbone stiffness of the studied polymer deviate strongly from those of polystyrene.

Table 1. Molecular weights, polydispersity, PS-βCD coverage, and synthetic yields

Sample	Color	SEC[a]		PS-βCD coverage[b] (%)	Yield (%)
		Mn	Mw/Mn		
3	orange	14600	1.46	-	43.1[c]
3c	yellow	19800	1.84	32	20.1

[a] Determined by GPC with polystyrene as standard. [b] Determined from ^{1}H-NMR spectra. [c,] Date taken from ref. 24

3.2. Optical properties

To display the photophysical behavior of **3** and **3c** compounds, their optical experiments were performed. All spectral data measurements are summarized in Table 2 and Figures 1 and 2. Both absorption and emission peaks of the two copolymers, **3** and **3c**, are clearly bathocromic shifted with respect to those of PF. This spectral shift can be understood in terms of the more planar backbone and the smaller band gap produced by the introduction of bithiophene as alternating repeating unit in the copolymers. The UV-Vis absorption maxima of compound **3** occurred at 443 nm (Figures 1b), while with the incorporation of PS-βCD macrocycle, for **3c**, a spectral broadening with a hypsochromic shift by ca. 16 nm was observed (Figure 1a). The hypsochromic shift could be attributed to a sterically driven increase in the twist angle (due to the inclusion of **3** inside the PS-βCD cavity) between adjacent fluorene chromophoric units on the polymer chain [17,24,33]. The emission spectra of **3** and **3c** displayed two peaks, at 495 and 528 nm and 496.5 and 521 nm, respectively corresponding to π-π* and n-π* transitions, as shown in (Figure 1c and 1d).

Table 2. Optical properties

Samples	solution λ_{max}(nm)[a]		film λ_{max}(nm)[b]		Eg (eV, UV/nm)[c]
	absorption	emission	absorption	emission	
3[d]	443	495, 528	451, 484	553, 575	2.32 (534)
3c	427	496.5, 521	440, 480	524	2.29 (541)

[a] Absorption and emission maxima in $CHCl_3$. [b] Absorption and emission maxima measured as film spin-coated from $CHCl_3$ solution. [c] The optical gap, Eg, estimated from the absorption onset (value in parentheses) of the UV-Vis spectrum of the polymer film ($Eg = 1240/\lambda_{onset}$). [d] Data taken from ref. 29

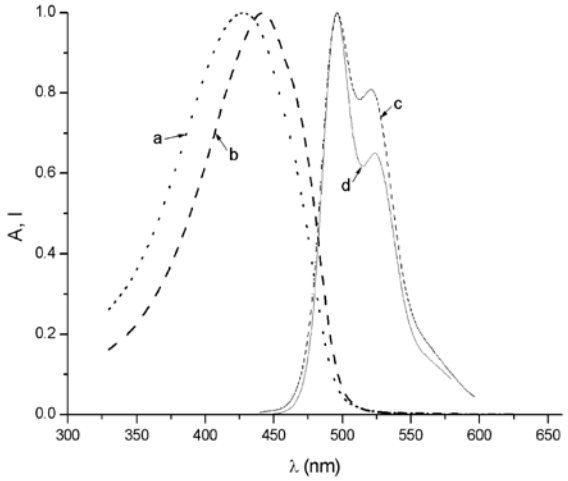

Fig. 1. Normalized absorption and fluorescence spectra of complexed 3c (a,c) and non-complexed 3 (b,d) in $CHCl_3$ solution.

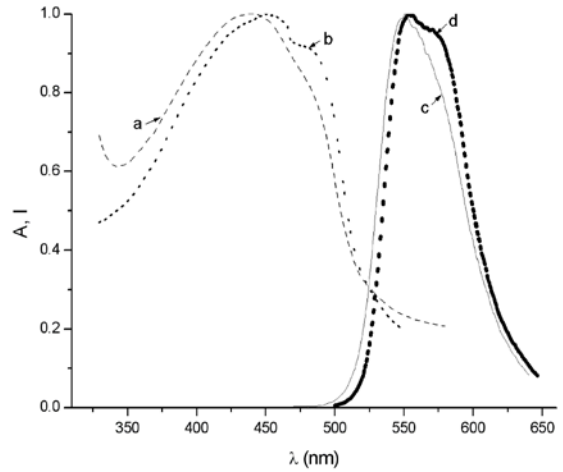

Fig. 2. Normalized UV-Vis absorption and fluorescence spectra of 3c (a, c) and 3 (b, d) film after annealed at 100 ^oC for 2 h.

The absorption and the emission spectra of the film state are more bathocromic shifted relative to solution stat ones, probably because of the increased intermolecular interactions between neighboring molecules in the film state. In the absorption spectrum of **3**, the absorption curve shows a maximum at 451 nm with small shoulder at 484 nm, (Figure 2b). A difference is observed on the spectrum of **3c** polyrotaxane, as shown in (Figure 2a), where the absorption curve shows a hypsochromic shift (maximum at 440 nm) with smaller shoulder at 480 nm. The maximum emission peak of copolymers is more bathocromic shifted upon spin coating from solution to the film state, indicating the polymer chains aggregation. It is noteworthy that the emission spectrum of **3c** is slightly sharper with one maximum peak at 524 nm (Figure 2c), compared with two maxima peaks at 553 and 575 nm of **3**, (Figure 2d). As observed for other polyrotaxanes, also in this case the emission spectrum of the **3c** polyrotaxane is blue shifted with respect to the non-rotaxane **3** copolymer which can be attributed to a reduction of intermolecular interactions or a sterically driven increase in twist angle between adjacent bithiophene units on the backbone [17]. Recently, comparison of threaded and unthreaded polymeric systems has allowed significant insights over the influence of threading on the emission properties of conjugated polymers and on the formation and the decay of interchain and intrachain excitonic species [17,24,33].

The optical band gap of **3** and **3c**, estimated from the absorption onset of the UV-Vis spectrum of the polymer film, approximately 2.32 and 2.29 eV, respectively is smaller than that of polyfluorene (PF) homopolymers.

3.3. Morphological properties

In order to determine the surface morphology and texture parameters of the non-rotaxane and rotaxane **3** and **3c** copolymers, AFM experiments were performed. They afforded the average height (μ) and root mean square roughness of the surfaces (*RMS*) as well as the grains average diameter (*D*), perimeter (P) and area (A), as shown in Table 3. The average diameter of the globular formations was calculated from the height profiles across each grain of the grains collected from the 5×5 μm^2 scan area for each sample. The 2D AFM images and a cross-section plot, along the solid line in the 2D height image were obtained for each sample, (Figures 3a and 4a).

Copolymer **3** showed globular formations and an agglomeration tendency with height (80-100 nm), whereas the **3c** sample showed a uniform and smooth surface, covered with individual small, spherically shaped formations, with a smaller height (~40 nm), (Figures 3c and 4c). As can be seen from the Table 3, the grains average diameter of **3** (157 nm) is smaller then that for the **3c** sample (412 nm).

Table 3. Roughness parametrs and characteristics of grains collected from 5 x 5 μm^2 AFM images.

Sample	Roughness Parameters		Grains Characteristics			
	μ (nm)[a]	*RMS*(nm)[b]	*No*[c]	*D*[d] (nm)	*P*[e] (nm)	*A*[f] (μm^2)
3	44.4	13.8	111	157	588	0.027
3c	28.7	8.9	23	412	1549	0.146

[a]Average height. [b]Root mean square roughness. [c]Number of grains collected. [d]Mean diameter of grains. [e] Mean perimeter of grains. [f] Mean area of grains.

The 3D AFM images provided further qualitative and quantitative information and showed the variable heights of the aggregates and globular formations, (Figures 3b and 4b). The average heights of the **3** and **3c** copolymers decrease from 44.4 nm to 28.7 nm, respectively. The trend toward a more uniform and smoother surface, already observed for the another rotaxane copolymers [24, 28] continues for the **3c** polymer rotaxane, where again an improvement of the *RMS* roughness can be observed, which is again superior to the properties of the uncomplexed polymer **3,** (Table 2). This provides microscopic evidence for strongly reduced interchain interactions, which allows the material to pack densely. The lower number of grains collected on the same scanning area (23) and the increases of grains average diameter, as well perimeter and area obtained for **3c** polyrotaxane can be another argument to the rotaxane formation.

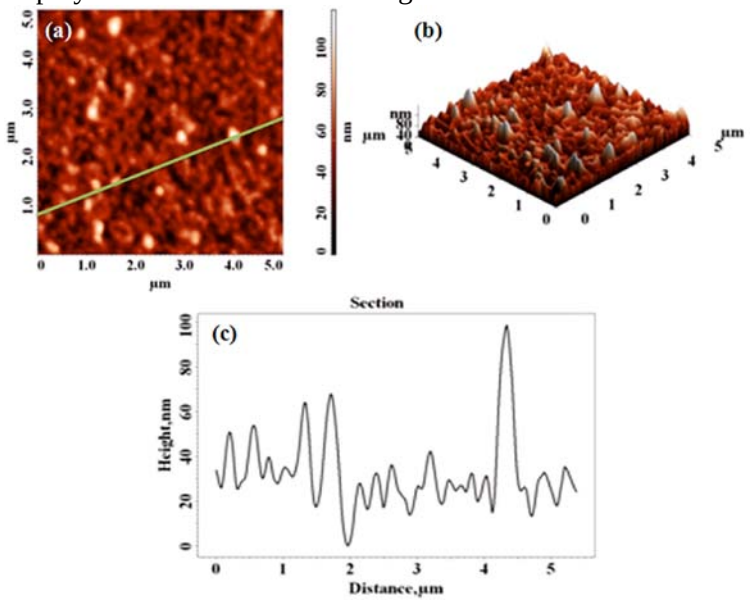

Fig. 3. 2D and 3D AFM topography images of non-complexed copolymer 3 (a, b) and the profile taken along the line in the 2D AFM image (c)

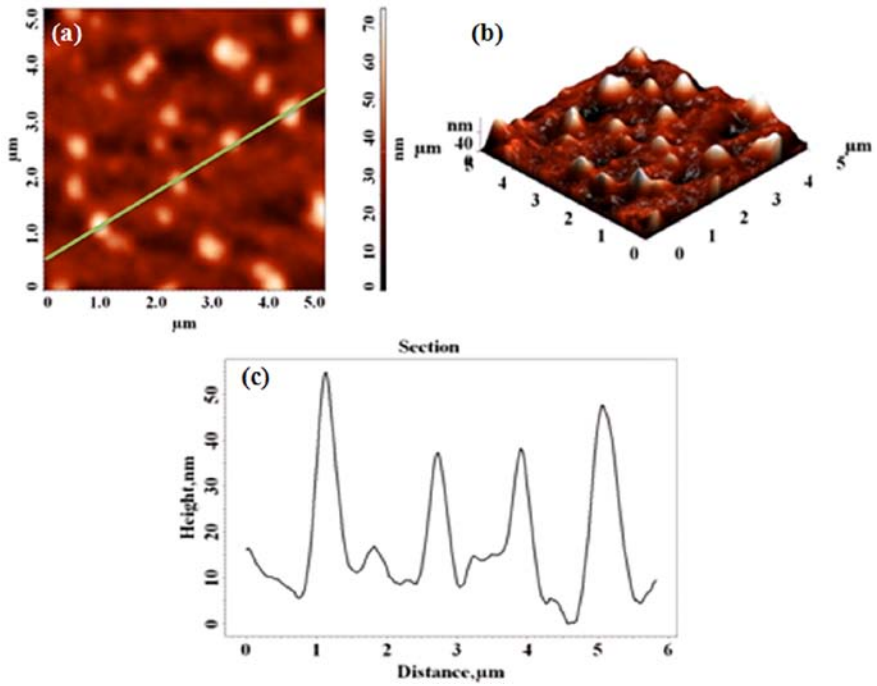

Fig. 4. 2D and 3D AFM topography images of polyrotaxane copolymer 3c (a, b) and the profile taken along the line in the 2D AFM image (c)

4. Discussion

The optimization of the material properties of organic conductors forms the foundation for the refinement of their applications. Generally, improvements of their optical properties and surface morphology are all desirable. Among possible approaches, the insulation of molecular wires by macrocyclic encapsulation (rotaxane formation) has a greater propensity to form ordered supramolecular assemblies [17-20]. With respect to the optical properties (Table 2), the emission spectra of the rotaxanes undergo a hypsochromic shift relative to the non-rotaxanes, which may be desirable for a particular application. More important, however, is the observed that the emission spectrum of **3c** is slightly sharper with one maximum peak, compared with two maxima peaks of **3** non-rotaxane ones (Figure 2d). AFM characterization (Table 3) demonstrate that **3c** rotaxane copolymer show more favorable surface parameters in comparison to **3** non-rotaxane copolymer (lower RMS roughness). In all cases, rotaxane formation improves the surface uniformity and good adhesivity on the glass slides. Important to note, the use of such polymeric materials in optoelectronics depends on the film forming ability as well as on the film-substrate interactions which usually produce characteristic morphological motifs.

5. Conclusions

We have demonstrated that the rotaxane formation has beneficial effects on optical properties and surface characteristics of conjugated polymers. The changes in the absorption and in the fluorescence properties occurred due to the presence of macrocycles, which is presumably related to a more rigid structure of the macromolecular chains. Rotaxane formation led also to an important modification on the rotaxane copolymers which show more favorable surface parameters compared with the non-rotaxane ones which was directly evidenced from AFM studies.

Acknowledgements

This work was supported by CNCSIS –UEFISCSU, project number PNII – IDEI cod 998/2008. Helpful cooperation of Dr. I. R. Tigoianu for UV-Vis measurements is acknowledged.

References

[1] A. J. Heeger, Angew. Chem., Int. Ed. **40**, 2591 (2001).
[2] L. Bürgi, T. Richards, R. Friend, and H. Sirringhaus, J. Appl. Phys. **94**, 6129 (2003).
[3] H. Hoppe, N. S. Sariciftci, J. Mater. Res. **19**, 1924 (2004).
[4] U. Scherf, E.J.W. List, Adv. Mater. **14**, 477 (2002).
[5] M. T. Bernius, M. Inbasekaran, J. O'Brien, W. S. Wu, Adv. Mater. **12**, 1737 (2000).
[6] J. H. Kim, H. Lee, Chem. Mater. **14**, 2270 (2002).
[8] R. Grisorio, P. Mastrorlli, C.F. Nobile, G. Romanazzi, G.P. Suranna, D. Acierno, E. Amendola, Macromol. Chem. Phys. **206**, 448 (2005).
[9] M. Beinhoff, A. T. Appapillai, L. D. Underwood, J. Frommer, K. R. Carter, Langmuir **22**, 2411 (2006).
[10] G. Zeng, W.-L. Yu, S.-J. Chua, W. Huang, Macromolecules **35**, 6907 (2002).
[11] B. Liu, W.-L. Yu, Y.-H. Lai, W. Huang, Macromolecules **33**, 8945 (2009).
[12] P. Blondin, J. Bouchard, S. Beaupre, M. Belletete, Macromolecules **33**, 5874 (2009).
[13] W. H. Tang, V. Chellappan, M. H. Liu, Z. K. Chen, L. Ke, ACS Appl. Mater. Interfaces, **1**, 1467 (2009).
[14] D. Zhao, W. H. Tang, L. Ke, S. T. Tan, X. W. Sun, ACS Appl. Mater. Interfaces **2**, 829 (2010).
[15] S. Brovelli, F. Cacialli, Small **6**, 2796 (2010).
[16] Y. Chen, Y.-M. Zhang, Y. Liu, Chem. Commun. **46** 5622 (2010).
[17] L. Zalewski, M. Wykes, S. Brovelli, M. Bonini, T. Breiner, M. Kastler, D. Dotz, D. Beljonne, H. L. Anderson, F. Caciali, P. Samori, Chem. Eur. J**. 16**, 3933 (2010).
[18] S. Brovelli, F. Meinardi, G. Winroth, O. Fenwick, G. Sforazzini, M. J. Frampton, L. Zalewski, J. A. Levitt, F. Marinello, P. Schiavuta, K. Suhling, H. L. Anderson, F. Caciali, Adv. Funct. Mater. **20**, 272 (2010).
[19] L. Zalewski, S. Brovelli, M. Bonini, J. M. Mativetsky, M. Wykes, E. Orgiu, T. Breiner, M. Kastler, F. Dötz, F. Meinardi, H. L. Anderson, D. Beljonne, F. Cacialli, P. Samori, Adv. Funct. Mater. **21**, 834 (2011).
[20] M. J. Frampton, H. L. Anderson, Angew. Chem. Int. Ed. **46**, 1028 (2007).
[21] M. Bonini, S. Rossi, G. Karlsson, M. Almgren, P. Lo Nostro, P. Baglioni, *Langmuir* **22**, 1478 (2006).
[22] G. Gonzalez-Gaitano, P. Rodriguez, J. R. Isasi, M. Fuentes, G. Tardajos, M. Sanchez, *J. Inclusion Phenomena Macrocyclic Chem.* **44**, 101 (2002).
[23] A. Farcas, N. Jarroux, P. Guegan, V. Harabagiu, V. Melnig, J. Optoelectronics Adv. Mater. **9**, 3484 (2007).
[24] A. Farcas, I. Ghosh, V. C. Grigoras, I. Stoica, C. Peptu, W. M. Nau, Macromol. Chem. Phys. **212**, 1022 (2011).
[25] A. Farcas, N. Jarroux, P. Guegan, A. Fifere, M. Pinteala, V. Harabagiu, J. Appl. Polym. Sci. **110**, 2384 (2008).
[26] A. Farcas, I. Ghosh, N. Jarroux, V. Harabagiu, P. Guegan, W. M. Nau, Chem. Phys. Lett. **465**, 96 (2008).
[27] A. Farcas, N. Jarroux, V. Harabagiu, P. Guegan, Eur. Polym. J. **45**, 795 (2009).
[28] A. Farcas, N. Jarroux, I. Ghosh, P. Guegan, W. M. Nau, V. Harabagiu, Macromol. Chem. Phys. **210**, 1440 (2009).
[29] A. Farcas, I. Stoica, A. Stefanache, C. Peptu, F. Farcas, N. Marangoci, L. Sacarescu, V. Harabagiu, P. Guégan, Chem. Phys. Lett. **508**, 111 (2011).
[30] A. Farcas, A. Fifere, I. Stoica, F. Farcas, A.-M. Resmerita Chem. Phys. Lett. CPLETT29535, DOI: 10.1016/j.cplett.2011.08.007.
[31] V. Harabagiu, B.C. Simionescu, M. Pinteala, C. Merrienne, J. Mahuteau, P. Guegan, H. Cheradame, Carbohyd. Polym. **56**, 301, (2004).
[32] A. Suzuki, J. Organomet. Chem. **576**, 147 (1999).
[33] F. Cacialli, J. S. Wilson, J. J. Michels, C. Daniel, C. Silva, R. H. Friend, N. Severin, P. Samori, J. P. Rabe, M. J. O'Connell, P. N. Taylor, H. L. Anderson, Nat. Mater. **1**, 160 (2002).